The Influence of Silicon in EN AW 6082 Alloys on the Bond Strength in Cold Pressure Welding

Christiane Gerlitzky,[1, a)] Siri Marthe Arbo,[2, b)] Ida Westermann,[2, c)] Peter Groche[1, d)]

[1]*Institute for Production Engineering and Forming Machines, Otto-Berndt-Straße 2, 64287 Darmstadt, Germany,*
[2]*Department of Materials Science and Engineering, Norwegian University of Science and Technology, Alfred Getz vei 2, NO-7491 Trondheim, Norway.*

a) Corresponding author: gerlitzky@ptu.tu-darmstadt.de
b) siri.m.arbo@ntnu.no c) ida.westermann@ntnu.no d) groche@ptu.tu-darmstadt.de

Abstract. Metallurgical joining of steel and aluminum has become a field of interest in research in the last years, as it will allow the production of load adapted lightweight components in the future. The production process of cold extrusion enables both, forming and joining at the same time obtaining high bond strengths in the final component. However, the reachable relative bond strength varies highly between different material combinations. This presented paper focuses on the influence of the silicon amount in EN AW 6082 and thus the influence on the reachable bond strength. The silicon content is varied between 0.7 and 1.3 wt%, while the magnesium content is kept constant at 0.6 wt %, which is within the range of the specifications of the commercially available alloy. Before joining the materials were aged to their T6 state, as well as a state of similar hardness despite the different silicon contents. The results show a significant influence of the silicon, as only joints produced with the material with higher silicon content reach bond strengths of 150 MPa. Differences of the material flow and hardness increase due to the deformation of the joined components were also observed. To further understand the mechanism behind these observations, FE-simulations were conducted to show the material flow and therefore, the reasons for the different strengths and geometries.

INTRODUCTION

Joining of dissimilar metals is of high importance for the automotive industry as it can facilitate the more intense usage of light weight metals, such as aluminum in car bodies, which can reduce the fuel consumptions and lower the environmental emissions [1, 2]. However, joining dissimilar metals, such as steel and aluminum is challenging due to the large differences in physical properties, such as strength, melting point and thermal expansion between the metals. In addition, the formation of brittle intermetallic phases, Fe_xAl_y, which can occur during the joining process must be taken into consideration [1–3]. In order to reduce the risk of intermetallic phase formation, joining must be performed at as low temperatures as possible using so called solid-state welding techniques.

Cold Pressure Welding (CPW) is a solid-state welding technique which utilize plastic deformation and high pressure in order to obtain a solid bond [4]. According to the bonding mechanism proposed by Bay [4], an equal amount of deformation between the metals is necessary in order to achieve areas where bonding occurs during cold pressure welding. However, if the difference in the strength between the metals to be joined is too different, unequal deformation can weaken the bond strength of the joint. It is stated by [5] that for joining dissimilar materials a similar strength of the two materials is essential. The reason however remains unclear.

The aluminum alloys in the 6xxx series are frequently used alloys in industry due to their excellent combinations of corrosion resistance and strength-to-weight ratio [6]. The main alloying elements in the 6xxx series are silicon, Si, and magnesium, Mg. It is especially suitable for investigations as the hardness and flow curves can be adapted easily by different heat treatments and composition of alloying elements. The alloys are classified as precipitation-hardenable aluminum alloys, meaning that with the correct heat treatment the Mg and Si atoms form Mg-Si precipitates (β'') within the structure, increasing the strength of the alloy to a maximum strength state, the T6 state [7]. The amount of Si and Mg in the alloy has a direct influence on the strength of the alloy [8], but for a given commercially available alloy the amount of the alloying elements might differ within a certain range. It is therefore important to know if small changes, even though the alloy classification is the same, result in differences in the bonding potential during CPW.

In this study the influence of the variations in Si content found in commercially available AA6082 aluminum alloy on the bonding potential when performing CPW with a steel component is investigated. The main focus is set on the influence of the alloys strengthening potential as a result of the varied Si content. The investigations include both experimental and numerical methods.

MATERIAL AND METHODS

Three cylindrical extruded aluminum alloys, all within the AA6082 classification were chosen for this study. The alloys contain various degrees of Si; 0.7 wt%, 1 wt% and 1.3 wt%, while the Mg content was kept constant at 0.6wt%. For steel, an extruded cylinder of 1.0401 steel was chosen in this study.

Prior to joining, the materials were heat treated. For the three aluminum alloys the heat treatment was chosen from the ageing curves to obtain the state with the highest hardness, the T6 state. Solution heat treatment was performed at 535°C in an air furnace for 1.5 hours for all the three alloys, followed by quenching. Thereafter a constant time gap of 30 minutes is kept before the aging. The alloys are aged to their individual T6 states. For comparison the Al1.0Si and Al1.3Si alloys are additionally aged to a state of similar hardness as Al0.7Si(T6). The aging process was performed at 195°C for various times depending on the desired hardness. The steel specimens were spherodized for five hours at 690°C. The chemical composition of the three aluminum alloys and the steel, as well as the hardness after the pre-heat treatments are presented in Table 1.

TABLE 1. Chemical composition of the alloys used in this study and the initial hardness obtained after heat treatment.

Materials	**Chemical composition [wt%]**								**Initial Hardness [HV 1]**
	Si	**Mg**	**Fe**	**Mn**	**Cr**	**Ti**	**Al**	**Other**	
Al0.7Si(T6)	0.67	0.57	0.20	0.51	0.145	0.02	97.86	Balance	80-85
Al1.0Si	0.96	0.56	0.20	0.51	0.146	0.02	97.57	Balance	80-85
Al1.0Si(T6)									100-105
Al1.3Si	1.28	0.57	0.20	0.49	0.156	0.04	97.22	Balance	80-85
Al1.3Si(T6)									110-115
	C	**Si**	**Mn**	**P**	**S**				
Steel C15	0.12-0.18	≤ 0.04	0.30-0.80	≤ 0.045	≤ 0.045				170

To further characterize the materials compression tests are performed with a "Zwick Roell 100kN" test machine. The initial mechanical properties before forming of all materials are measured after the heat treatments using samples with a 10 mm diameter and 15 mm height according to [9]. The resulting stress-strain curves (FIGURE 1) are imported into the simulations after the correction of the machine stiffness. They are further utilized for the simulations to get a deeper understanding of the local bonding conditions. The simulations are conducted with "DEFORM Integrated 2D3D", which is a commercially available simulation program specialized on the high deformation occurring in bulk forming as in extrusion processes. Especially the factors surface enlargement, normal pressure and relative movement are important parameters influencing the bonding. These parameters can easily be read out from the simulation results but are hardly measurable in the experiments. The tools are modeled as elastic, whereas the workpieces are modeled as plastic bodies. For the friction the shear model was used as the Coulomb model can result in unrealistic shear stresses if high pressures occur as they are typical in cold forming [10]. The friction factor m was defined as 0.4 for to the aluminum - tool contact and 0.08 for the steel - tool contact according to the DEFORM pre-settings. The contact between the aluminum and steel samples was chosen as 0.9 since this should simulate the high friction, which occurs when bonds form. The flow curves of the different materials are shown in figure 1. Depending on the amount of excess Si a different hardening potential is noticed. It should be noted that the three specimens A1.0Si, A1.0Si(T6) and Al1.3Si show a different behavior at strains below 0.3, until they result in similar curves at large strains. Figure 1 b) on the other hand shows the process steps of the CPW process. Cylindrical specimens with a diameter of 41.5 mm and height 15 mm where turned, then coated and brushed directly before the joining process. For the cold pressure welding process, the surface preparation prior to joining is crucial. In this study, the brushing technique used [11] was chosen to enhance the bonding [12]. After the brushing, the joining of the two cylinders to an extruded cup was completed within 10 minutes [13]. The brushing force was set to 75 N and the surfaces were brushed back and forth in three 120° shifted directions. These parameters were found suitable during preliminary testing. These parameters differ from earlier investigations in [13] due to the lower hardness of the materials used in this study.

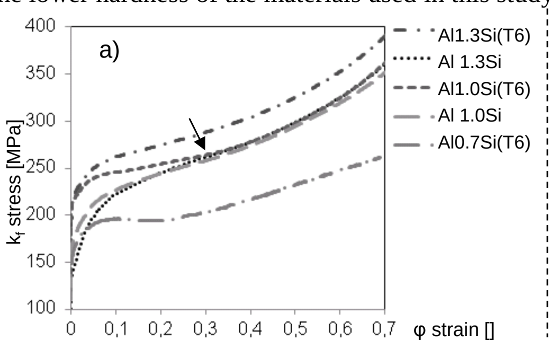

FIGURE 1. Stress stain curve for aluminum materials (a) and process steps (b).

The joined specimens were cut in half and following ground and polished in order to study the interface characteristics. After tensile testing of the joints, the fracture surfaces are additionally studied using scanning electron microscopy (SEM) combined with energy-dispersive X-ray spectroscopy (EDS) in order to study the fracture mechanism. The SEM settings are set to a 10 kV electron beam in high current mode, 10.5 mm working distance and an aperture of 60 µm. The different flow behavior could however not be visualized in the microstructure of the samples after joining as the grain refinement and material flow is similar between all the aluminum materials. In all the alloys, independent of chemical composition and initial hardness, a fine grained microstructure could be observed in the center region of the joints with clear elongated grains in the outer areas. Vickers hardness with 1 kp load was obtained for both the steel and aluminum alloys before and after joining to quantify the cold hardening.

RESULTS AND DISCUSSIONS

After joining, the samples were cut in half in order to study the interface between steel and aluminum at a macroscopic level. Images of the cross-sections of the joined samples are shown in Figure 2, presenting the joints of the different aluminum alloys and the resulting various material flows. The red lines show the resulting material flow determined in simulations. In the joints produced with the harder aluminum alloys the localized thinning of the steel in the center of the joints is most prominent and shows a clear difference in the material flow, compared to the joints made with aluminum in a softer initial state. This phenomenon cannot be rebuilt in the simulations. The reason for the big deviations between the experiments and the simulations in the center of the specimens can be explained with the high normal pressures. In the center region there is a hydrostatic stress state which reduces to the outer areas (see fig. 2 right). According to [14] this hydrostatic stress state can increase the flow stress by up to 15%. This seems not to be taken into account by the simulation software. Also the surface enlargement and contact normal pressures are relatively similar between the materials; therefore, they are not further described in this paper.

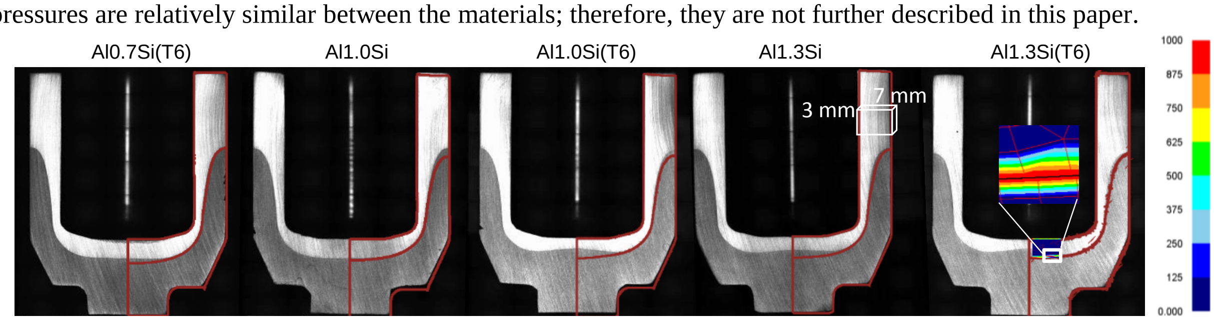

FIGURE 2. Images show the cross-sections of the joined samples with the different aluminum alloys in their different initial states. The red lines show the resulting material flow predicted by the simulations. Right: the contact pressures in the center region are pictured.

The details about the local tribological loads can be taken out of the simulation results but the numerical model cannot predict the resulting bond strength. For this reason 3 mm thick slices were cut out of the center of the samples in order to evaluate how the different material flows affects the bond strength of the joints. Following they were tensile tested and the measured force is divided by the cross sectional area as described in [13]. This area measures 3 mm x 7 mm (see fig. 2). The results for the joined samples are shown in Figure 3 (a). The lowest measured bond strength was obtained for the joints produced with the weakest aluminum alloy, Al0.7Si(T6). In general, higher bond strength is achieved for the joints produced with the aluminum alloys which have a higher strength prior to joining. However, the joints produced with Al1.3Si(T6) differs from this trend. It should be noted that the brushing parameters described earlier where chosen constant for comparison reasons. They were obtained for the alloys Al0.7Si(T6) and Al1.0Si(T6) in pretests and then kept for the main experiments. The Al1.3Si(T6) alloy, however, resembles the samples used in our previous work, which where the optimal brushing parameters for the commercially available EN AW 6082. Therefore, it is assumed that the effect by the brushing was not successful.

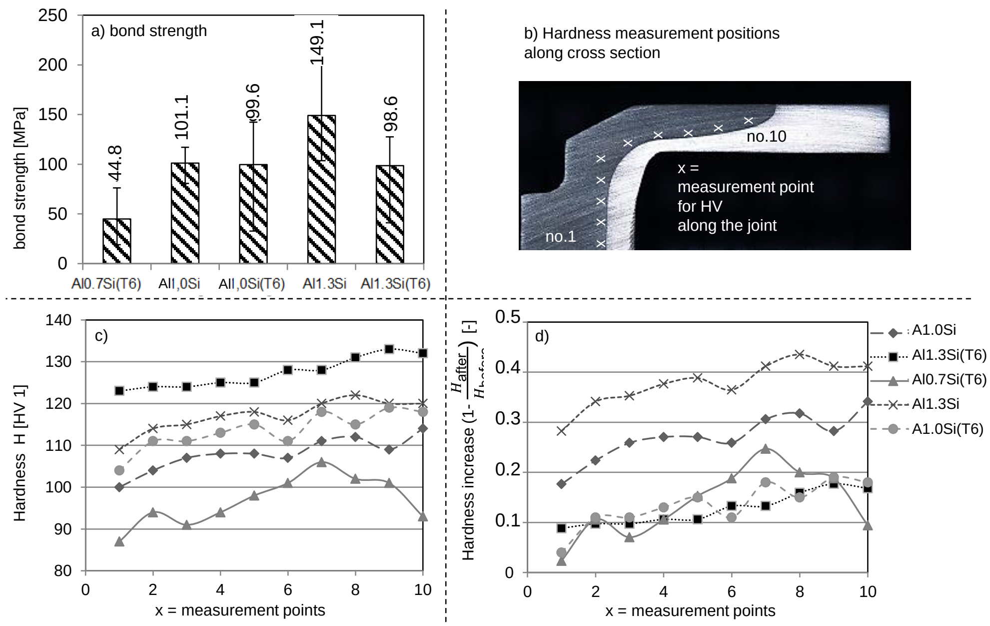

FIGURE 3. Bond strengths (a), hardness measurement positions (b), hardness (c) and relative hardness increase (d) after joining.

The measured hardness (positions see fig. 3 b) is presented in Figure 3 (c) showing the hardness after joining. The hardness in the bonded aluminum can be written in the following sequence, from lowest to highest hardness; Al0.7Si(T6) - Al1.0Si - Al1.0Si(T6) - Al1.3Si - Al1.3Si(T6) which is nearly the same order as the bond strengths. In figure 3 (d) the relative hardness increase after joining along the bond is calculated. In the three cases where the aluminum was aged to T6 prior to joining, a similar hardness increase during the joining process is observed (see fig. 2 (d)). This hardness increase is a result of the work hardening experienced by the aluminum during the large plastic deformations introduced during the joining process. In the joints where the aluminum alloys were in a softer under aged state prior to joining, the aluminum samples have obtained the largest increases in hardness. These under aged alloys contain Si and Mg in solid solution. The excess Si in solute solution is known to improve the work hardening effect which occurs during the joining process [8, 15]. The high relative hardness increase observed in the aluminum is also the reason, that the final material flow of the initially soft Al1.3Si resembles that of the initially hard Al1.3Si(T6) (see figure 2). This leads to the finding that the initial hardness does not necessarily need to be high. If the hardness is strongly different to the one of the joining partner, the hardening potential needs to be available during the forming process. Both an initial hardness as well as a high and early hardness increase is visible for the samples with Al1.0Si - Al1.0Si(T6) can result in good bond strengths. However, it should be taken into account to adjust the brushing parameters with respect to the initial hardness.

To underline these results and get a deeper understanding of how the solid bond was achieved, the fracture surfaces were studied using SEM combined with EDS mapping. Special focus was set to detecting residual aluminum on the steel fracture surfaces. The area of the steel where the material flows around the punch was analyzed (see figure 4 d)). This is also the area of the joints where the final fracture occurs during tensile testing. Therefore, the highest bond strength is located at this position. From the analysis of the steel fracture surfaces, residual aluminum was observed for all joined samples. Figure 4, shows the residual aluminum (black) detected on the steel fracture surface from (a) a Al0.7Si(T6) sample with a measured bond strength of 40 MPa, while (b) is for a Al1.0Si sample with a measured bond strength of 120 MPa. However, no clear difference in the amount of residual aluminum on the surfaces can be observed. Therefore, for these samples it can be assumed that there is no correlation between the amount of the residual aluminum and the resulting bond strength. This relationship can typically be observed for cold pressure welding by rolling, where hardly any relative movement is observed during joining and the residual metal found on the surface can be used as a measurement for bond strength. [16]. Naseri et al. [16] used a trilayered aluminum composite, or materials with the same flow curves, which leads to an even deformation and inhibits or even eliminates relative movement.

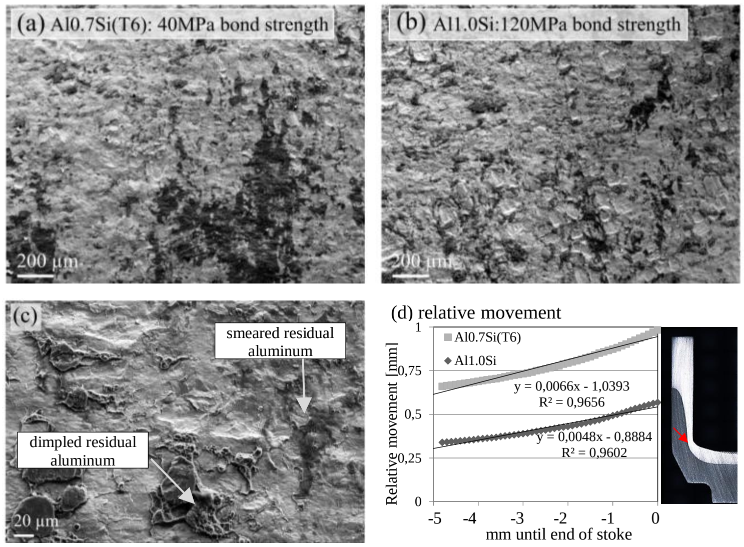

FIGURE 4. SEM images of the steel fracture surfaces where the residual aluminum is shown in black for sample joined with Al0.7Si(T6) (a) sample joined with Al1.0Si. Image (b) shows a high magnification of the characteristics of the residual aluminum, smeared or with dimples(c). shows the relative movement at the analyzed position of the highest bond strength(d).

The assumption, that high relative movement can destroy the earlier established bonds is verified by the calculation of the relative movement between the steel to the aluminum side. The data is taken from the numerical model at the position of the highest bond strength (see figure 4 d). This relative movement is analyzed by measuring how far two points, which are initially at the same position move apart. In Figure 4 d) the results for the two materials shown in a) and b) are pictured as well as a linear regression for each. It can be noted that the absolute relative movement in the section of the highest bond strength is higher for the material Al0.7Si(T6) as well as the gradient (slope = 0.0066 mm). A higher difference in the initial hardness and no potential of hardness increase therefore leads to a high relative movement and a higher gradient at the end of the forming process. This however is crucial since most of the bond strength is established w[5].

Additionally, the residual aluminum observed shows two different characteristics, see Figure 4 (c). Some of the residual aluminum has a clear topography and contains small dimples, indicating a ductile fracture. The rest of the aluminum was in the form of a thin layer, which looked as if it was smeared out on the steel surface. This finding supports that this type of residual aluminum is a result of the relative movement occurring during the joining process and bonding perhaps had occurred at one point, but got broken during the continuous joining process. It therefore does not participate to the final bond strength measured in the tensile tests. This is why we suggest that a direct relationship between the amount of residual aluminum and the bond strength should not be assumed. Further, if the material strength of the joining partners vary, a SEM analysis with high resolution needs to be performed. A correlation to the characteristics of the ductile residual aluminum would be of high interest but can only finally be verified with very time consuming SEM analysis of the complete fracture surface of many samples.

SUMMARY AND CONCLUSIONS

In this study, the influence on the amount of Si in the commercially available AA6082 on the bonding potential between aluminum and steel by CPW was investigated by experimental and numerical analysis. The effect of the initial mechanical properties of the aluminum alloys, including the effect of having excess Si in the structure, on the bonding potential have been analyzed. The results show that the initial hardness or the hardening potential of the aluminum needs to be close to the hardness of the steel joining partner to establish a stronger bond. The thinning of the steel sample in the center of the joints can be related to the increase in hardness in the aluminum alloy during the joining process. It was shown that a higher amount of excess Si leads to a higher hardness increase after the joining process. Another observation is that the residual aluminum on the steel fracture surface cannot be used as parameter to predict the bond strength. It was underlined with the gradient of the relative movement derived from the simulations. This is the reason why it should be taken into consideration if joining material of different strengths that the deformation is unequal and, therefore, a relative movement between the joining partners weakens the bond. The relative movement breaks bonds that have been established at an earlier stage in the joining process. This finding was supported by the observations of the residual aluminum found on the steel fracture surfaces, which had two different characteristics. However, it is suggested, that dimpled residual aluminum indicates a ductile fracture contributing to the achieved bond strength.

ACKNOWLEDGEMENTS

The authors gratefully acknowledge the DFG (Deutsche Forschungsgemeinschaft) for the financial support of the subproject “Investigation and enhancement of bonding by cold bulk metal forming processes” (GR 1818/48-3) within priority program 1640 “Joining by plastic deformation”. In addition the work presented in this study is based on research activity within SFI Manufacturing in Norway partially funded by the Research Council of Norway (contract number 237900).

REFERENCES

1. ©European Aluminium Association: EAA Aluminium Automotive Manual EAA Aluminium Automotive Manual - Joining : 11. Joining dissimilar materials, 2015
2. Atabaki, M. Mazar ; Nikodinovski, M. ; Chenier, P. ; Ma, J. ; Harooni, M. ; Kovacevic, R.: Welding of Aluminum Alloys to Steels: An Overview. In: Journal for Manufacturing Science and Production (2014), Nr. 2
3. Springer, H. ; Kostka, A. ; Payton, E. J. ; Raabe, D. ; Kaysser-Pyzalla, A. ; Eggeler, G.: On the formation and growth of intermetallic phases during interdiffusion between low-carbon steel and aluminum alloys. In: Acta Materialia 59 (2011), Nr. 4, S. 1586–1600
4. Bay, N.: Cold Pressure Welding—The Mechanisms Governing Bonding. In: Journal of Engineering for Industry 101 (1979), Nr. 2, S. 121
5. Wohletz, Simon: Erzeugung stoffschlüssiger Verbunde durch Kaltfließpressschweißen. 1. Auflage. Herzogenrath : Shaker, 2017 (Berichte aus Produktion und Umformtechnik 105)
6. Friis, Jesper ; Holmedal, Bjørn ; Ryen, Øyvind ; Nes, Erik ; Myhr, Ole R. ; Grong, Øystein ; Furu, Trond ; Marthinsen, Knut: Work Hardening Behaviour of Heat-Treatable Al-Mg-Si-Alloys. In: Materials Science Forum (2006), S. 519–521
7. Smallman, R. E.: Modern Physical Metallurgy (8th ed.). Amsterdam : Butterworth-Heinemann, 2014
8. Gupta, A. K. ; Lloyd, D. J. ; Court, S. A.: Precipitation hardening in Al–Mg–Si alloys with and without excess Si. In: Materials Science and Engineering: A 316 (2001), 1-2, S. 11–17
9. DIN 50106:2016-11: Prüfung metallischer Werkstoffe - Druckversuch bei Raumtemperatur, 2016-11
10. K. Pöhlandt, D. Banabic, K. Lange: On the determination of friction coefficients by ring compression (2004), III. URL www.UTFscience.de
11. Haats, Joachim: Verfahrensoptimierung beim Kaltpreßschweißen artverschiedener korrosionsbeständiger Metalle. Als Ms. gedr. Düsseldorf : VDI-Verl., 1994 (Fortschrittberichte VDI / 2 305)
12. Bay, N. ; Clemensen, C. ; Juelstorp, O. ; Wanheim, T.: Bond Strength in Cold Roll Bonding. In: CIRP Annals - Manufacturing Technology 34 (1985), Nr. 1, S. 221–224
13. Gerlitzky, Christiane ; Volz, Stefan ; Groche, Peter: Brushing for High Performance Cold Pressure Welded Bonds. In: Key Engineering Materials 767 (2018), S. 309–315
14. Bridgman, P. W.: Studies in Large Plastic Flow and Fracture. Cambridge : Harvard University Press, 1964
15. Zhao, Qinglong ; Holmedal, Bjørn: The effect of silicon on the strengthening and work hardening of aluminum at room temperature. In: Materials Science and Engineering: A 563 (2013), S. 147–151
16. Naseri, M. ; Reihanian, M. ; Borhani, E.: Bonding behavior during cold roll-cladding of tri-layered Al/brass/Al composite. In: Journal of Manufacturing Processes 24 (2016), S. 125–137